Generalized nondipole strong-field approximation of high-order harmonic generation

Björn Minneker,[1,2,3,*] Birger Böning,[2,3,†] and Stephan Fritzsche[1,2,3]
[1]*Theoretisch-Physikalisches Institut, Friedrich-Schiller-Universität Jena, D-07743 Jena, Germany*
[2]*Helmholtz-Institut Jena, D-07743 Jena, Germany*
[3]*GSI Helmholtzzentrum für Schwerionenforschung GmbH, D-64291 Darmstadt, Germany*

(Received 2 June 2022; accepted 17 October 2022; published 10 November 2022)

The strong-field approximation (SFA) is a widely used theoretical framework that describes the process of high-order harmonic generation of atoms and molecules. Here, we propose a generalization of the dipole SFA towards weakly relativistic contributions to the laser-electron interaction. These weakly relativistic contributions are closely related to the spatial structure of the light field and imply a correction of the relativistic order $1/c$. Within this generalized nondipole SFA (GN-SFA), we demonstrate how to obtain explicit results and discuss their physical aspects. This approach enables one to investigate the nondipole effects of linear polarized plane waves as well as the influence of structured light fields, such as twisted light, that have not yet been captured by the currently available models. In order to utilize our generalized nondipole SFA, we consider a linearly polarized plane wave and demonstrate the decrease of the harmonic yield that is directly related to the nondipole effects of the laser field. Furthermore, we discuss the GN-SFA with regard to other nondipole SFA approaches by determining their physical and mathematical context. Finally, the GN-SFA is a powerful theoretical framework that extends the nonrelativistic SFA rigorously to the weakly relativistic regime and therefore will be a useful model for further theoretical investigations.

DOI: 10.1103/PhysRevA.106.053109

I. INTRODUCTION

In the past decades, atomic processes in strong laser fields have attracted much attention. In particular, strong-field ionization [1–3] and high-order harmonic generation (HHG) [4–9] have led to insights into the electron dynamics in such light fields. Several applications like pump-probe experiments have benefited from extremely short pulses. These short pulses have a large spectral width which, in the context of high-order harmonic generation, is associated with very high-order harmonic orders q [10]. However, in order to understand and utilize such high orders, the present nonrelativistic models need to be extended toward weakly relativistic electron dynamics.

From a theoretical perspective, ongoing research in the topic of strong-field physics led to different approaches to solve the time-dependent Schrödinger equation (TDSE). Apart from numerical solutions, nowadays, one of the most successful approaches to solve the TDSE is the strong-field approximation (SFA [11,12]). The standard form of the SFA requires analytic solutions of continuum states of an electron in the intense driving laser field that neglects the comparably weak atomic potential. Under this assumption, the continuum solutions to the TDSE are the well-known Volkov states which initially were constructed as the solution of the fully relativistic Dirac equation [13]. The nonrelativistic version of the Volkov state is also called the dipole Volkov state. This dipole Volkov state is mathematically defined to have the form of a plane wave with an additional purely time-dependent phase briefly referred to as the Volkov phase. The resulting *dipole* or *nonrelativistic* SFA has been thoroughly compared to HHG experiments and found valid for a broad range of parameters. Nevertheless, driving laser fields have recently approached the limits of such nonrelativistic models. Thus it is necessary to extend these models also towards the (weak) relativistic regime of the electron dynamics. In particular, such an extension of the dipole SFA is also known as a nondipole SFA. Recent theoretical models [14,15] include weakly relativistic contributions by expanding the potential of the respective laser fields in the Hamiltonian. While a perturbative approach seems to be useful, where the laser field is approximated already in the Hamiltonian, such a treatment is limited to purely monochromatic driving laser beams. Furthermore, twisted laser fields like Laguerre Gaussian beams or Bessel beams cannot be studied without proper consideration of their spatial structure.

Therefore, in this work, we generalize the nondipole strong-field approximation by incorporating analytically accurate Volkov states that include all relevant weakly relativistic contributions of the laser field. In contrast to previous approaches, the developed nondipole SFA allows one to consider also more complicated beam arrangements and is *not* limited to single plane waves. Therefore, we cannot only incorporate an arbitrary number of laser fields but also account for the corresponding individual weakly relativistic contributions. The nondipole SFA developed in this work is valid for the same set of laser field configurations that can be treated within the dipole SFA. Accordingly, it constitutes a generalization of the dipole SFA into the weakly relativistic

*bjoern.minneker@uni-jena.de
†b.boening@posteo.de

 ©2022 American Physical Society

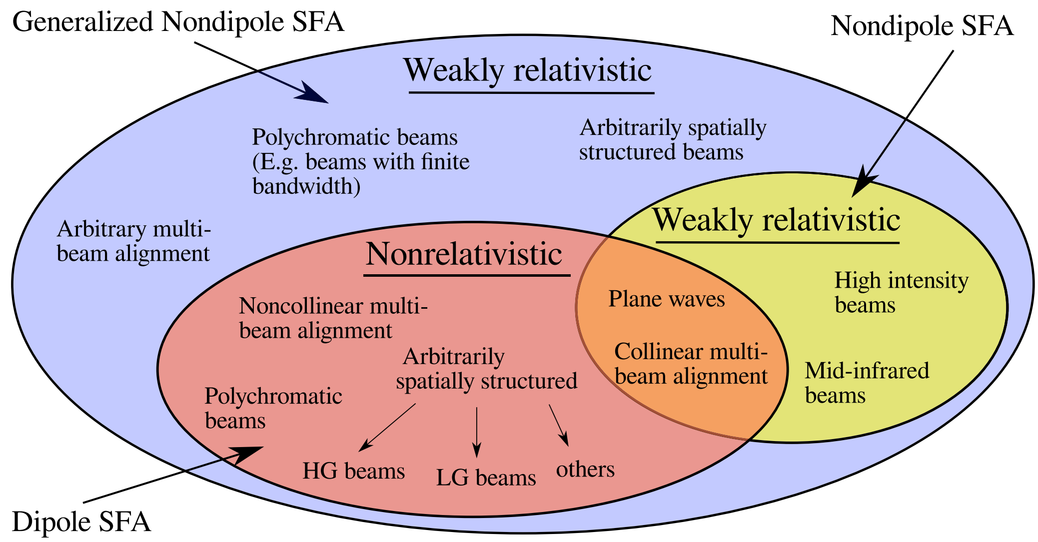

FIG. 1. Physical configurations that can be described by the dipole SFA (red ellipse), nondipole SFA (yellow ellipse), and the generalized nondipole SFA (blue ellipse). The terms which appear twice differ only in their interval of validity concerning non- and weakly relativistic effects.

regime, See Fig. 1. Henceforth, we refer to it as the *generalized nondipole SFA* (GN-SFA). As in the standard dipole SFA, several microscopic and macroscopic effects like phase matching or ground-state depletion are not explicitly considered in this work. While further investigations are necessary to incorporate these effects into the GN-SFA, the general results presented in this work will not be altered.

This paper is structured as follows. In Sec. II we derive the general formalism and final results of the GN-SFA. In more detail, Sec. II A considers a gauge covariant formulation of the nondipole strong-field amplitude and Sec. II B decouples and reformulates the analytic solution of the nondipole Volkov state. Subsequently, in Sec. II C we derive the general formula for the dipole moment and in Sec. II D the developed model is applied to an elliptically polarized plane wave. Furthermore, in Sec. III A we discuss the GN-SFA by comparing it to a standard variant of the nondipole SFA. In order to utilize the GN-SFA, we apply it to a linearly polarized plane wave and discuss the decrease of the harmonic yield in relation to the dipole SFA. Finally, we conclude our findings in Sec. IV.

In the following, we use atomic units ($\hbar = e = m_e = 4\pi\epsilon_0 = 1$) unless stated otherwise.

II. THEORETICAL MODEL

To derive a generalized nondipole SFA (GN-SFA), we begin with the general Coulomb-gauge Hamiltonian of an electron in the combined potential of an atomic core and an intense laser field. The associated time-dependent Schrödinger equation (TDSE) is written as

$$i\hat{\partial}_t \Psi(\boldsymbol{r}, t) = \hat{\mathcal{H}}\Psi(\boldsymbol{r}, t), \tag{1}$$

where $\hat{\partial}_t$ denotes the partial derivative with respect to t. The Hamiltonian reads

$$\hat{\mathcal{H}} = \frac{[\hat{\boldsymbol{p}} - q\boldsymbol{A}(\boldsymbol{r}, t)]^2}{2} + \hat{V}(\boldsymbol{r}) + q\Phi(\boldsymbol{r}, t), \tag{2}$$

with the atomic binding potential $\hat{V}(\boldsymbol{r})$, the momentum operator of the electron $\hat{\boldsymbol{p}}$, and its charge $q = -1$ for electrons. $\boldsymbol{A}(\boldsymbol{r}, t)$ and $\Phi(\boldsymbol{r}, t)$ are the vector and scalar potentials of the laser field, respectively. To follow the internal logic of Sec. II A it is beneficial to review the basic concept of the dipole SFA.

The dipole SFA is an approximation which is widely used in strong-field physics and can be summarized by a few standard assumptions [16] as follows.

(1) The strong laser field does not couple with any bound state beyond the ground state.

(2) The amplitude of the ground state, $a(t)$, is considered to be known.

(3) The continuum states are described by Volkov states which neglect contributions of the atomic potential.

These assumptions simplify the model extensively and allow for analytical treatment. On the other hand, they directly affect the gauge freedom in such a way that the resulting physical observable of interest, the atomic dipole moment, is not necessarily gauge covariant anymore [17]. Especially the ionization and recombination amplitude from the bound state into the dressed continuum and vice versa are gauge dependent, which induces the breakdown of the gauge covariance. Fortunately, the gauge covariance in the dipole SFA can be guaranteed by a careful treatment of the Hamiltonian and its associated time-evolution operators [18]. Since the nondipole SFA requires similar assumptions as the dipole SFA we demonstrate that the associated nondipole amplitudes are also gauge covariant within such treatment.

A. Gauge covariance of the nondipole SFA

The standard form of the dipole SFA is formulated in the so-called length gauge where the gauge freedom allows a vanishing vector potential $\boldsymbol{A}(t) \equiv 0$. In accordance with the dipole SFA, many of the standard nondipole SFA theories [14,15,19] are formulated in length gauge. This choice of gauge is reasonable since the electromagnetic potentials in the Hamiltonian $\boldsymbol{A}(\boldsymbol{r},t)$ and $\Phi(\boldsymbol{r},t)$ can be simply expanded up to the first relativistic order $\frac{|\boldsymbol{k}|}{\omega_k} = \frac{1}{c}$. Here $\boldsymbol{k} = |\boldsymbol{k}|\boldsymbol{e_k}$ is the momentum vector of the electromagnetic potentials, ω_k the frequency, and c the speed of light. Unfortunately, it is not possible to treat the laser field in length gauge if its concrete (spatial) shape is taken to be arbitrary, since it is necessary to develop a corresponding theoretical framework in the so-called velocity gauge which is characterized by the gauge condition $\Phi(\boldsymbol{r},t) \equiv 0$. To provide a gauge covariant theory, we follow the idea of Klaiber *et al.* [20] and later from Becker and Milosevic [18,21] in the dipole regime and extend the formalism to weakly relativistic (nondipole) laser fields.

One of the crucial steps to define a proper gauge covariant nondipole SFA is the definition of the time-evolution operator

$$|\Psi(t)\rangle = \hat{U}(t,t_0)\,|\Psi(t_0)\rangle\,,$$

where $\hat{U}(t,t_0)$ evolves the wave function Ψ from time t_0 to t, with $t_0 \leqslant t$. As a consequence (of this definition), the time-evolution operator of a general Hamiltonian $\mathcal{H}_j(t)$ follows the Schrödinger equation

$$i\hat{\partial}_t\hat{U}_j(t,t_0) = \hat{\mathcal{H}}_j(t)\hat{U}_j(t,t_0).$$

To actually calculate the time-evolution operator of the Hamiltonian (2), it is convenient to split the Hamiltonian into two parts

$$\hat{\mathcal{H}} = \hat{\mathcal{H}}_A + \hat{\mathcal{H}}_B,$$

and use a Dyson series such that

$$\hat{U}(t,t_0) = \hat{U}_A(t,t_0) - i\int_{t_0}^{t} dt'\hat{U}(t,t')\hat{\mathcal{H}}_B(t')\hat{U}_A(t',t_0), \quad (3)$$

where $\hat{U}_A(t,t_0)$ is the time-evolution operator associated with the Hamiltonian $\hat{\mathcal{H}}_A(t)$. To achieve a gauge-covariant nondipole SFA, we set $\hat{\mathcal{H}}_A$ and $\hat{\mathcal{H}}_B$ to

$$\hat{\mathcal{H}}_A = \hat{\xi} - q\boldsymbol{r}\cdot\hat{\partial}_t\boldsymbol{A}(\boldsymbol{r},t), \quad (4a)$$

$$\hat{\mathcal{H}}_B = q\big[\Phi(\boldsymbol{r},t) + \boldsymbol{r}\cdot\hat{\partial}_t\boldsymbol{A}(\boldsymbol{r},t)\big], \quad (4b)$$

where the *energy operator* $\hat{\xi}$ is defined as

$$\hat{\xi} = \frac{[\hat{\boldsymbol{p}} - q\boldsymbol{A}(\boldsymbol{r},t)]^2}{2} + \hat{V}(\boldsymbol{r}),$$

$$i\hat{\partial}_t\hat{U}_\xi(t,t_0) = \hat{\xi}(t)\hat{U}_\xi(t,t_0), \quad \Rightarrow \hat{\mathcal{H}} = \hat{\xi} + q\Phi(\boldsymbol{r},t). \quad (5)$$

Note that Eq. (5) is only correct in Coulomb gauge $\hat{\nabla}\cdot\boldsymbol{A}(\boldsymbol{r},t) = 0$, which is incorporated by the Coulomb gauge Hamiltonian (2). Inserting the Hamiltonian (4b) into the Dyson series (3) leads to an explicit expression for the full time-evolution operator

$$\hat{U}(t,t_0) = \hat{U}_A(t,t_0) - i\int_{t_0}^{t} dt'\hat{U}(t,t') \times q[\Phi(t') + \boldsymbol{r}\cdot\hat{\partial}_{t'}\boldsymbol{A}(\boldsymbol{r},t')]\hat{U}_A(t',t_0),$$

with

$$i\hat{\partial}_t\hat{U}_A(t,t_0) = [\hat{\xi} - q\boldsymbol{r}\cdot\hat{\partial}_t\boldsymbol{A}(\boldsymbol{r},t)]\hat{U}_A(t,t_0)$$

as the operator corresponding to the Hamiltonian Eq. (4a).

The gauge covariance can best be understood in the context of above-threshold ionization. There, in particular, the so-called direct SFA transition amplitude is given by

$$M_{\boldsymbol{p}} = \lim_{t\to\infty,\,t_0\to-\infty} \langle\Psi_{\boldsymbol{p}}(t)|\,\hat{U}(t,t_0)\,|\Psi_g(t_0)\rangle\,.$$

The final gauge-covariant ionization amplitude is defined by

$$M_{\boldsymbol{p}} = -i\int_{-\infty}^{\infty} dt'\,\langle\chi_{\boldsymbol{p}}(\boldsymbol{r},t')|\,e^{-iq\boldsymbol{r}\cdot\boldsymbol{A}(\boldsymbol{r},t')} \times q[\Phi(\boldsymbol{r},t') + \boldsymbol{r}\cdot\hat{\partial}_{t'}\boldsymbol{A}(\boldsymbol{r},t')]\,|\Psi_g(t')\rangle\,, \quad (6)$$

with the Volkov states $\chi_{\boldsymbol{p}}(\boldsymbol{r},t)$ [22,23]. The gauge covariance in the dipole regime is seen immediately if we choose either length gauge $\Phi(t) = 0$ or velocity gauge $\boldsymbol{A}(t) = 0$. The missing phase term $q\boldsymbol{r}\boldsymbol{A}(t)$ in the velocity-gauge Volkov state is compensated by the exponential factor in front of the Volkov state in Eq. (6). However, in velocity gauge, the scalar potential vanishes in the absence of free charges, such that the ionization amplitude reads

$$M_{\boldsymbol{p}} = iq\int_{\infty}^{\infty} dt'\,\langle\chi_{\boldsymbol{p}}(\boldsymbol{r},t')|\,e^{-iq\boldsymbol{r}\cdot\boldsymbol{A}(\boldsymbol{r},t')}\boldsymbol{r}\cdot\boldsymbol{E}(\boldsymbol{r},t')\,|\Psi_g(t')\rangle\,.$$

The high-order harmonic process, described within the SFA, is based on the ionization amplitudes and its complex conjugation discussed in this section. Therefore, we can make use of this gauge invariance of the direct ionization amplitudes to also apply to high-order harmonic generation.

B. Nondipole Volkov states

In this subsection we will discuss the spatially structured nondipole Volkov state $\chi_{\boldsymbol{p}}(\boldsymbol{r},t)$ [22,23] and derive an adaption with which we can formulate a generalization of the nondipole SFA.

In general the Volkov state is the solution of the TDSE for a charged particle in an external electromagnetic field,

$$\hat{\mathcal{H}}_{le} = \frac{[\hat{\boldsymbol{p}} - q\boldsymbol{A}(\boldsymbol{r},t)]^2}{2}. \quad (7)$$

For electrons with $q = -1$ the Hamiltonian is referred to as the laser-electron Hamiltonian. In the context of the SFA, the atomic binding potential $V(\boldsymbol{r})$ is omitted since the interaction with the electron in the continuum results in a minor correction [16]. The resulting TDSE reads

$$i\hat{\partial}_t\chi_{\boldsymbol{p}}(\boldsymbol{r},t) = \frac{[\hat{\boldsymbol{p}} + \boldsymbol{A}(\boldsymbol{r},t)]^2}{2}\chi_{\boldsymbol{p}}(\boldsymbol{r},t) = \frac{1}{2}[\hat{\nabla}^2 - 2i\boldsymbol{A}(\boldsymbol{r},t)\cdot\hat{\nabla} + \boldsymbol{A}^2(\boldsymbol{r},t)]\chi_{\boldsymbol{p}}(\boldsymbol{r},t), \quad (8)$$

with a quite general vector potential defined by [23]

$$\boldsymbol{A}(\boldsymbol{r},t) = \int d^3\boldsymbol{k}\,\boldsymbol{A}_{\boldsymbol{k}}^R(t) = \int d^3\boldsymbol{k}\,\mathrm{Re}[\boldsymbol{a}_{\boldsymbol{k}}e^{iu_{\boldsymbol{k}}}]. \quad (9)$$

In this expression, the radial and temporal dependencies of the vector potential are imprinted in the phase $u_{\boldsymbol{k}} = \boldsymbol{k}\cdot\boldsymbol{r} - \omega_{\boldsymbol{k}}t$. Finally, the continuum states are given by [23]

$$\chi_{\boldsymbol{p}}(\boldsymbol{r},t) = \frac{1}{(2\pi)^{3/2}}e^{-i(E_{\boldsymbol{p}}t - \boldsymbol{p}\cdot\boldsymbol{r}) - i\Gamma(\boldsymbol{r},t)}, \quad (10)$$

with $E_p = \boldsymbol{p}^2/2$ and the nondipole Volkov phase $\Gamma(\boldsymbol{r}, t)$, which is explicitly given by Eq. (A2) in Appendix A. The precise form of the nondipole Volkov phase depends on the explicit structure of the vector potential, defined in terms of $\boldsymbol{a}_{\boldsymbol{k}}$, and needs to be evaluated for any specific case of interest.

A key technique to evaluate SFA amplitudes is the so-called saddle-point approximation (see Sec. II C below). This requires the separation of the spatial and temporal contributions $\boldsymbol{k}\cdot\boldsymbol{r}$ and $\omega_{\boldsymbol{k}}t$, which is still possible for arbitrary laser field geometries. In the following, we demonstrate the decomposition for a general term of the nondipole Volkov phase Eq. (A2) that can be expressed as

$$\Gamma_i(\boldsymbol{r}, t) = \int d^3\boldsymbol{k}'\, \nu^{(i)}_{\boldsymbol{k}\boldsymbol{k}'} \sin\left(u_{\boldsymbol{k}'} + \Omega^{(i)}_{\boldsymbol{k}\boldsymbol{k}'}\right), \tag{11}$$

where $\nu^{(i)}_{\boldsymbol{k}\boldsymbol{k}'}$ and $\Omega^{(i)}_{\boldsymbol{k}\boldsymbol{k}'}$ do not depend on $\boldsymbol{r}$ or t. Equation (11) can be rewritten as

$$\begin{aligned}\Gamma_i(\boldsymbol{r}, t) = &\int d^3\boldsymbol{k}'\, \nu^{(i)}_{\boldsymbol{k}\boldsymbol{k}'} \cos\left(\omega_{\boldsymbol{k}'}t - \Omega^{(i)}_{\boldsymbol{k}\boldsymbol{k}'}\right)\sin(\boldsymbol{k}'\boldsymbol{r})\\ &- \int d^3\boldsymbol{k}'\, \nu^{(i)}_{\boldsymbol{k}\boldsymbol{k}'} \sin\left(\omega_{\boldsymbol{k}'}t - \Omega^{(i)}_{\boldsymbol{k}\boldsymbol{k}'}\right)\cos(\boldsymbol{k}'\boldsymbol{r}).\end{aligned} \tag{12}$$

Here, we can Taylor expand the trigonometric functions around zero with regard to $\boldsymbol{k}'\cdot\boldsymbol{r}$. This expansion can either be done before or after the momentum integration without loss of accuracy. After expanding the trigonometric functions, $\boldsymbol{k}'\cdot\boldsymbol{r}$ can always be written as $|\boldsymbol{r}||\boldsymbol{k}'|\cos(\phi_{\boldsymbol{r}\boldsymbol{k}'})$. Shifting $|\boldsymbol{r}|^j$ out of the integral allows one to assign to each term of the expansion a specific fixed value that depends on the power j. Since this representation is still exact and the integrand is independent of $\boldsymbol{r}$, the result for each order needs to agree with the scenario in which the integration was done before the Taylor expansion. However, we want to demonstrate the general procedure of the decomposition, which is done explicitly for the first term in Eq. (12):

$$\begin{aligned}&\int d^3\boldsymbol{k}'\, \nu_{\boldsymbol{k}\boldsymbol{k}'} \cos(\omega_{\boldsymbol{k}'}t - \Omega_{\boldsymbol{k}\boldsymbol{k}'})\sin(\boldsymbol{k}'\cdot\boldsymbol{r})\\ &= \sum_{j=0}^{\infty} \frac{(-1)^j}{(2j+1)!}\left(\frac{1}{c}\right)^{2j+1}\\ &\quad\times \int d^3\boldsymbol{k}'\, \nu_{\boldsymbol{k}\boldsymbol{k}'}\omega_{\boldsymbol{k}'}^{2j+1} \cos(\omega_{\boldsymbol{k}'}t - \Omega_{\boldsymbol{k}\boldsymbol{k}'})(\boldsymbol{e}_{\boldsymbol{k}'}\cdot\boldsymbol{r})^{2j+1}.\end{aligned}$$

Since we work within the framework of the (nonrelativistic) Schrödinger equation, the contributions of terms in the Taylor expansion decrease quickly with increasing order j. This rapid decrease allows one to neglect all contributions beyond the linear order ($1/c \Leftrightarrow \boldsymbol{k}'\cdot\boldsymbol{r}$). With that in mind, the approximation of Eq. (12) reads

$$\begin{aligned}\Gamma_i(\boldsymbol{r}, t) &\approx \boldsymbol{r}\cdot\boldsymbol{\Gamma}^{(r)}_i(t) + \Gamma^{(t)}_i(t)\\ &= \boldsymbol{r}\cdot \int d^3\boldsymbol{k}'\, \nu^{(i)}_{\boldsymbol{k}\boldsymbol{k}'} \cos\left(\omega_{\boldsymbol{k}'}t - \Omega^{(i)}_{\boldsymbol{k}\boldsymbol{k}'}\right)\boldsymbol{k}'\\ &\quad - \int d^3\boldsymbol{k}'\, \nu^{(i)}_{\boldsymbol{k}\boldsymbol{k}'} \sin\left(\omega_{\boldsymbol{k}'}t - \Omega^{(i)}_{\boldsymbol{k}\boldsymbol{k}'}\right)\\ &= \int d^3\boldsymbol{k}'\, \nu^{(i)}_{\boldsymbol{k}\boldsymbol{k}'}\left(\boldsymbol{k}'\cdot\boldsymbol{r} + \frac{1}{\omega_{\boldsymbol{k}'}}\hat{\partial}_t\right)\cos\left(\omega_{\boldsymbol{k}'}t - \Omega^{(i)}_{\boldsymbol{k}\boldsymbol{k}'}\right).\end{aligned}$$

Nevertheless, it can be seen clearly that the only $\boldsymbol{r}$ independent part is associated with the Taylor expansion of the cosine term ($j = 0$). This explicitly demonstrates that only terms of the form $\cos(\boldsymbol{k}'\cdot\boldsymbol{r})$ assign an $\boldsymbol{r}$ independent contribution.

Following the above logic, every term in the nondipole Volkov phase Eq. (A2) can be approximated. Therefore, this procedure can be applied to *any physical laser field* within the limitations of the model itself. As a result, the full nondipole Volkov phase can be written in the form

$$\Gamma(\boldsymbol{r}, t) \approx \sum_i \boldsymbol{r}\cdot\boldsymbol{\Gamma}^{(r)}_i(t) + \Gamma^{(t)}_i(t) = \boldsymbol{r}\cdot\boldsymbol{\Gamma}^{(r)}(t) + \Gamma^{(t)}(t).$$

Moreover, it is convenient to reformulate $\Gamma^{(t)}(t)$ to perform a saddle-point approximation

$$\Gamma^{(t)}(t) = \boldsymbol{p}\cdot\boldsymbol{\Gamma}_{\boldsymbol{p}}(t) + \Gamma_{\boldsymbol{A}}(t), \tag{13}$$

where the subscript $\boldsymbol{p}$ denotes a particle-field contribution and the subscript $\boldsymbol{A}$ a field-field contribution.

C. High harmonic generation in the nondipole SFA

Harmonic radiation is the dipole radiation emitted by a recombining electron with its parent ion. It is defined by its dipole moment

$$\boldsymbol{D}(t) = \langle\Psi(t)|\,\hat{\boldsymbol{r}}\,|\Psi(t)\rangle\,, \tag{14}$$

with the wave function

$$\begin{aligned}|\Psi(t)\rangle &= \hat{U}_\xi(t, t_0)\,|\Psi_g(t_0)\rangle\\ &\quad - i\int_{t_0}^{t} dt'\hat{U}(t, t')\hat{V}_\xi(t')\hat{U}_\xi(t', t_0)\,|\Psi_g(t_0)\rangle\\ &= e^{iq\boldsymbol{r}\cdot\boldsymbol{A}(\boldsymbol{r},t)}\,|\Psi_g(t)\rangle\\ &\quad - i\int_{t_0}^{t} dt'\hat{U}(t, t')\hat{V}_\xi(t')e^{iq\boldsymbol{r}\cdot\boldsymbol{A}(\boldsymbol{r},t')}\,|\Psi_g(t')\rangle\,.\end{aligned} \tag{15}$$

The explicit form and definition of the components in this equation were discussed in Sec. II A. Inserting this wave function into the dipole moment (14) yields

$$\begin{aligned}\boldsymbol{D}(t) = -i\int_{t_0}^{t} dt'\,&\langle\Psi_g(t)|\,e^{i\boldsymbol{r}\cdot\boldsymbol{A}(\boldsymbol{r},t)}\boldsymbol{r}\hat{U}(t, t')\hat{V}_\xi(t')\\ &\times e^{-i\boldsymbol{r}\cdot\boldsymbol{A}(\boldsymbol{r},t')}\,|\Psi_g(t')\rangle\,,\end{aligned}$$

where continuum-continuum transitions (process of higher order) are neglected. Furthermore, the interaction operator $\hat{V}_\xi(t')$ can be written in velocity gauge as

$$\begin{aligned}\hat{V}_\xi(t') &= -[\Phi(t') + \boldsymbol{r}\cdot\hat{\partial}_{t'}\boldsymbol{A}(\boldsymbol{r}, t')]\\ \overset{\Phi(t')\equiv 0}{\Rightarrow}\ \hat{V}_\xi(t') &= -\boldsymbol{r}\cdot\hat{\partial}_{t'}\boldsymbol{A}(\boldsymbol{r}, t')\\ &= \boldsymbol{r}\cdot\boldsymbol{E}(\boldsymbol{r}, t').\end{aligned}$$

Similar to the dipole SFA, we neglected the atomic core potential in the continuum which reduces the general time-evolution operator $\hat{U}(t, t_0)$ to the time-evolution operator of the dressed electron

$$\hat{U}_{le}(t, t_0) = \int d^3\boldsymbol{p}\,|\chi_{\boldsymbol{p}}(\boldsymbol{r}, t)\rangle\,\langle\chi_{\boldsymbol{p}}(\boldsymbol{r}, t_0)|\,. \tag{16}$$

Note that the time-evolution operator in Eq. (16) is constructed from the spatially structured nondipole Volkov states in Eq. (10). With this in mind the dipole moment reads

$$\begin{aligned}\boldsymbol{D}(t) &= -i\int_{-\infty}^{t} dt' \int d^3\boldsymbol{p}\, \langle\Psi_g(t)|\, e^{i\boldsymbol{r}\cdot\boldsymbol{A}(\boldsymbol{r},t)}\boldsymbol{r}\,|\chi_{\boldsymbol{p}}(\boldsymbol{r},t)\rangle\\ &\quad\times \langle\chi_{\boldsymbol{p}}(\boldsymbol{r},t')|\,\boldsymbol{r}\cdot\boldsymbol{E}(\boldsymbol{r},t')e^{-i\boldsymbol{r}\cdot\boldsymbol{A}(\boldsymbol{r},t')}\,|\Psi_g(t')\rangle\\ &= -i\int_{-\infty}^{t} dt' \int d^3\boldsymbol{p}\, \langle\Psi_g(t)|\,\boldsymbol{r}\,|\boldsymbol{\pi}(\boldsymbol{p},\boldsymbol{r},t)\rangle\\ &\quad\times \langle\boldsymbol{\pi}(\boldsymbol{p},\boldsymbol{r},t')|\,\boldsymbol{r}\cdot\boldsymbol{E}(\boldsymbol{r},t')\,|\Psi_g(t')\rangle\\ &\quad\times e^{-i\int_{t'}^{t} d\tau\left[E_{\boldsymbol{p}}+\hat{\partial}_\tau\Gamma^{(t)}(\tau)\right]}, \end{aligned}\tag{17}$$

with $\boldsymbol{\pi}(\boldsymbol{p},\boldsymbol{r},t) = \boldsymbol{p}+\boldsymbol{A}(\boldsymbol{r},t)-\boldsymbol{\Gamma}^{(r)}(t)$. This always holds for eigenstates of the atomic Hamiltonian, not only for hydrogenlike ones. However, to analytically proceed further we restrict the atomic species to be hydrogenlike such that $|\Psi_g(t)\rangle = |\Psi_g\rangle\, e^{iI_p t}$ holds and the ground state is known. This assumption allows one to calculate the matrix elements in Eq. (17) analytically. We define the *nondipole matrix element* in Eq. (17) as

$$\begin{aligned}\boldsymbol{\Upsilon}(\boldsymbol{\pi}(\boldsymbol{p},t)) &= \langle\boldsymbol{\pi}(\boldsymbol{p},\boldsymbol{r},t)|\,\boldsymbol{r}\,|\Psi_g\rangle\\ &= \left\{i\hat{\partial}_\beta\hat{\partial}_\gamma\left[\boldsymbol{d}\left(\boldsymbol{\pi}^{(R)}_{\beta\gamma}(\boldsymbol{p},t)\right)-\boldsymbol{d}\left(\boldsymbol{\pi}^{(I)}_{\beta\gamma}(\boldsymbol{p},t)\right)\right]\right.\\ &\quad\left.+\boldsymbol{d}(\boldsymbol{\pi}(\boldsymbol{p},t))\right\}_{\beta=\gamma=0}+O(1/c^2),\end{aligned}\tag{18}$$

with

$$\begin{aligned}\boldsymbol{A}(t) &= \boldsymbol{A}(\boldsymbol{r},t)|_{\boldsymbol{k}\cdot\boldsymbol{r}=0},\\ \boldsymbol{\pi}^{(i)}_{\beta\gamma}(\boldsymbol{p},t) &= \boldsymbol{p}+\boldsymbol{A}(t)-\boldsymbol{\Gamma}^{(r)}(t)+\boldsymbol{a}^i_0\beta+\boldsymbol{\kappa}^i(t)\gamma,\\ \boldsymbol{\pi}(\boldsymbol{p},t) &= \boldsymbol{\pi}^{(i)}_{00}(\boldsymbol{p},t).\end{aligned}$$

Note that in the standard nondipole SFA $\boldsymbol{\pi}(\boldsymbol{p},t)$ is usually referred to as the kinetic momentum of the electron, while $\hat{\partial}_\beta\hat{\partial}_\gamma\boldsymbol{d}(\boldsymbol{\pi}^{(R)}_{\beta\gamma}(\boldsymbol{p},t))$ can be found in Eq. (B7) in Appendix B with the dummy variables β and γ. Furthermore, $\boldsymbol{a}_0$ is the zeroth-order (nonrelativistic) contribution of the Taylor expansion of $\boldsymbol{a_k}$ with respect to $\boldsymbol{k}$ and $\delta_{\boldsymbol{k}}$ denotes the nonpolynomial contributions like delta distributions. The superscripts I and R represent the imaginary and real parts, respectively, and $(i)\in\{(R),(I)\}$ is an index of $\boldsymbol{\pi}^{(i)}_{\beta\gamma}(\boldsymbol{p},t)$. Note that $\boldsymbol{A}(t)\equiv\boldsymbol{A}(\boldsymbol{r},t)|_{\boldsymbol{k}\cdot\boldsymbol{r}=0}$ is equal to the dipole vector potential. We define

$$\begin{aligned}\boldsymbol{A}(\boldsymbol{r},t) &= \boldsymbol{A}^R(t)+\mathrm{Re}[\boldsymbol{a}_0(\boldsymbol{r}\cdot\boldsymbol{\kappa}(t))]+O(1/c^2)\\ &\approx \boldsymbol{A}(t)+\boldsymbol{a}^R_0(\boldsymbol{r}\cdot\boldsymbol{\kappa}^R(t))-\boldsymbol{a}^I_0(\boldsymbol{r}\cdot\boldsymbol{\kappa}^I(t)),\\ \boldsymbol{\kappa}(t) &= i\int d^3\boldsymbol{k}\,\delta_{\boldsymbol{k}}\boldsymbol{k}\,e^{-i\omega_{\boldsymbol{k}}t},\end{aligned}$$

where $\boldsymbol{\kappa}(t)$ contributes only if the spectral bandwidth of the laser field is small. The nondipole ionization amplitude in the dipole moment (17) can be calculated within a similar approach to be

$$\begin{aligned}\langle\boldsymbol{\pi}(\boldsymbol{p},\boldsymbol{r},t')|\,\boldsymbol{r}\cdot\boldsymbol{E}(\boldsymbol{r},t')\,|\Psi_g\rangle &= [\boldsymbol{E}(t')\cdot\boldsymbol{\Upsilon}(\boldsymbol{\pi}(\boldsymbol{p},t'))-\Lambda(\boldsymbol{p},t')]\\ &\quad+O(1/c^2),\end{aligned}\tag{21}$$

$$\begin{aligned}\Lambda(\boldsymbol{p},t') = \hat{\partial}_\beta\big([\hat{\partial}_{t'}\boldsymbol{\kappa}^R(t')]\cdot\boldsymbol{d}\big(\boldsymbol{\pi}^{(R)}_{\beta\gamma}(\boldsymbol{p},t')\big)\\ -[\hat{\partial}_{t'}\boldsymbol{\kappa}^I(t')]\cdot\boldsymbol{d}\big(\boldsymbol{\pi}^{(I)}_{\beta\gamma}(\boldsymbol{p},t')\big)\big)\big|_{\beta=\gamma=0},\end{aligned}\tag{22}$$

where $\hat{\partial}_\beta\boldsymbol{d}(\boldsymbol{\pi}^{(i)}_{\beta\gamma}(\boldsymbol{p},t'))$ is defined in Eq. (B6) in Appendix B. Note that, in $\Lambda(\boldsymbol{p},t')$ as defined in Eq. (22), we get an additional term in the ionization amplitude compared to the dipole regime which is associated with the spatial dependent contribution of the electric field $\boldsymbol{E}(\boldsymbol{r},t')$. However, inserting Eqs. (18) and (21) into the dipole moment (17) yields

$$\begin{aligned}\boldsymbol{D}(t) &= -i\int_{-\infty}^{t} dt'\int d^3\boldsymbol{p}\,\boldsymbol{\Upsilon}^*(\boldsymbol{\pi}(\boldsymbol{p},t))\\ &\quad\times[\boldsymbol{E}(t')\cdot\boldsymbol{\Upsilon}(\boldsymbol{\pi}(\boldsymbol{p},t'))-\Lambda(\boldsymbol{p},t')]e^{-iS(\boldsymbol{p},t',t)},\end{aligned}\tag{23}$$

$$S(\boldsymbol{p},t',t) = \int_{t'}^{t} d\tau[E_{\boldsymbol{p}}+\hat{\partial}_\tau\Gamma^{(t)}(\tau)+I_p].\tag{24}$$

Using Eq. (13), the argument of the action S reads

$$E_{\boldsymbol{p}}+\hat{\partial}_\tau\Gamma^{(t)}(\tau)+I_p = \tfrac{p^2}{2}+\boldsymbol{p}\cdot\hat{\partial}_\tau\boldsymbol{\Gamma}_{\boldsymbol{p}}(\tau)+\hat{\partial}_\tau\tilde{\Gamma}_{\boldsymbol{A}}(\tau)+I_p.$$

To evaluate the crucial contributions to the momentum integral in Eq. (23), we perform a saddle-point approximation of the momentum integral. The momentum needs to obey the saddle-point condition such that

$$\begin{aligned}\boldsymbol{0} &= \hat{\nabla}_{\boldsymbol{p}}S = \hat{\nabla}_{\boldsymbol{p}}\int_{t'}^{t} d\tau[E_p+\hat{\partial}_\tau\Gamma^{(t)}(\tau)+I_p],\\ \boldsymbol{0} &= \int_{t'}^{t} d\tau\,\boldsymbol{p}_s[1+\hat{\partial}_\tau(\nabla_{\boldsymbol{p}}\cdot\boldsymbol{\Gamma}_{\boldsymbol{p}})]+\hat{\partial}_\tau(\boldsymbol{\Gamma}_{\boldsymbol{p}}+\hat{\nabla}_{\boldsymbol{p}}\cdot\Gamma_{\boldsymbol{A}}),\end{aligned}\tag{25}$$

where $\boldsymbol{\Gamma}_{\boldsymbol{p}}$ and $\Gamma_{\boldsymbol{A}}$ defined in Eq. (13) can be decomposed as

$$\boldsymbol{p}\cdot\boldsymbol{\Gamma}_{\boldsymbol{p}} = \Gamma^{(t)}_1+\Gamma^{(t)}_3,\quad \Gamma_{\boldsymbol{A}} = \Gamma^{(t)}_2+\Gamma^{(t)}_4+\Gamma^{(t)}_5.$$

In the dipole SFA $\Gamma^{(t)}_1$ and $\Gamma^{(t)}_2$ are associated with the physical contributions $\boldsymbol{p}\cdot\boldsymbol{A}(t)$ and $\boldsymbol{A}(t)^2$, respectively. The contributions $\Gamma^{(t)}_i$ for $i\in\{3,4,5\}$ are the respective weakly relativistic corrections in the nondipole SFA. Since $\boldsymbol{\Gamma}_{\boldsymbol{p}}$ and $\Gamma_{\boldsymbol{A}}$ are still momentum dependent due to the factor $\eta_{\boldsymbol{k}}$, the solution of the saddle-point equation (25) is nontrivial. Taylor expanding $\eta_{\boldsymbol{k}}$ allows one to iteratively solve Eq. (25) to an arbitrary order of accuracy with the ansatz $\boldsymbol{p}=\sum_{i=0}^{\infty}\boldsymbol{p}_i$ and $\boldsymbol{p}_i\propto 1/c^i$. However, since our model only accounts for corrections up to $1/c$ in Eq. (25) the general saddle-point momentum $\boldsymbol{p}_s$ results as

$$\boldsymbol{p}_s(t,t')\equiv\boldsymbol{p}_s = \boldsymbol{p}_0+\frac{1}{t-t'}\left[\int d^3\boldsymbol{k}\,\boldsymbol{k}\frac{\left[\boldsymbol{p}_0\cdot\boldsymbol{A}^I_{\boldsymbol{k}}(\tau)\right]}{\omega^2_{\boldsymbol{k}}}+\boldsymbol{A}^I_{\boldsymbol{k}}(\tau)\frac{(\boldsymbol{p}_0\cdot\boldsymbol{k})}{\omega_{\boldsymbol{k}}}-\boldsymbol{I}(\tau)\right]^{t}_{\tau=t'},\tag{27a}$$

$$\boldsymbol{I}(t) = \int d^3\boldsymbol{k}\int d^3\boldsymbol{k}'\left(\frac{\omega_{\boldsymbol{k}'}\boldsymbol{A}^R_{\boldsymbol{k}}(t)\left[\boldsymbol{k}\cdot\boldsymbol{A}^I_{\boldsymbol{k}'}(t)\right]-\omega_{\boldsymbol{k}}\boldsymbol{A}^I_{\boldsymbol{k}}(t)\left[\boldsymbol{k}\cdot\boldsymbol{A}^R_{\boldsymbol{k}'}(t)\right]}{\omega_{\boldsymbol{k}}(\omega^2_{\boldsymbol{k}}-\omega^2_{\boldsymbol{k}'})}+\frac{\left[2\omega_{\boldsymbol{k}}\omega_{\boldsymbol{k}'}\boldsymbol{k}'-(\omega^2_{\boldsymbol{k}}+\omega^2_{\boldsymbol{k}'})\boldsymbol{k}\right]\left[\boldsymbol{A}^R_{\boldsymbol{k}}(t)\cdot\boldsymbol{A}^I_{\boldsymbol{k}'}(t)\right]}{(\omega^2_{\boldsymbol{k}}-\omega^2_{\boldsymbol{k}'})^2}\right),\tag{27b}$$

with the nonrelativistic saddle-point momentum

$$\boldsymbol{p}_0(t,t') \equiv \boldsymbol{p}_0 = \frac{1}{t-t'}\int d^3k \frac{\boldsymbol{A}^I_{\boldsymbol{k}}(\tau)}{\omega_{\boldsymbol{k}}}\bigg|_{\tau=t'}^{t} = -\frac{1}{t-t'}\int_{t'}^{t} d\tau\, \boldsymbol{A}^R(\tau). \quad (28)$$

Note that both denominators in Eq. (27b) can induce singularities. For specific laser field configurations it is beneficial to reformulate the real and imaginary parts of the vector potential similarly to Eq. (A2) and integrate the remaining $\boldsymbol{k}$ and $\boldsymbol{k}'$ dependent expression.

After performing the saddle-point approximation the dipole momentum reads

$$\boldsymbol{D}(t) = -i\int_{-\infty}^{t} dt' \sqrt{\frac{(2\pi i)^3}{|\boldsymbol{H}_{\boldsymbol{p}}(S)|}}\Bigg|_{\boldsymbol{p}=\boldsymbol{p}_s} \times [\boldsymbol{E}(t')\cdot\boldsymbol{\Upsilon}(\boldsymbol{\pi}(\boldsymbol{p}_s,t')) - \Lambda(\boldsymbol{p}_s,t')] \times \boldsymbol{\Upsilon}^*(\boldsymbol{\pi}(\boldsymbol{p}_s,t))e^{-iS(\boldsymbol{p}_s,t',t)}, \quad (29)$$

where $\boldsymbol{H}_{\boldsymbol{p}}(S)$ is the Hessian matrix of the action S Eq. (24) with respect to the momentum $\boldsymbol{p}$. Fourier transforming Eq. (29) yields the induced atomic dipole momentum of the harmonic order q

$$\boldsymbol{D}(\omega_q) = -i\int_{-\infty}^{\infty} dt \int_{-\infty}^{t} dt' \sqrt{\frac{(2\pi i)^3}{|\boldsymbol{H}_{\boldsymbol{p}}(S)|}}\Bigg|_{\boldsymbol{p}=\boldsymbol{p}_s} \times [\boldsymbol{E}(t')\cdot\boldsymbol{\Upsilon}(\boldsymbol{\pi}(\boldsymbol{p}_s,t')) - \Lambda(\boldsymbol{p}_s,t')] \times \boldsymbol{\Upsilon}^*(\boldsymbol{\pi}(\boldsymbol{p}_s,t))e^{-i\Theta(\boldsymbol{p}_s,t',t)}, \quad (30)$$

with $\Theta(\boldsymbol{p}_s,t',t) = \int_{t'}^{t} d\tau[E_{\boldsymbol{p}_s} + \hat{\partial}_\tau\Gamma^{(t)}(\tau) + I_p] - \omega_q t$. The remaining temporal integrals can again be evaluated using saddle-point approximations, where t and t' obey the saddle-point equations

$$\hat{\partial}_{t/t'}\Theta(\boldsymbol{p}_s,t',t) = 0, \quad \Rightarrow E_{\boldsymbol{p}_s} + \hat{\partial}_t\Gamma^{(t)}(t_s) = \omega_q - I_p,$$
$$\Rightarrow E_{\boldsymbol{p}_s} + \hat{\partial}_{t'}\Gamma^{(t)}(t'_s) = -I_p.$$

The final expression of the dipole moment $\boldsymbol{D}(\omega_q)$ then reads

$$\boldsymbol{D}(\omega_q) = -i\sum_s \sqrt{\frac{(2\pi i)^5}{|\boldsymbol{H}_{t,t'}(S)||\boldsymbol{H}_{\boldsymbol{p}}(S)|}}\Bigg|_{(\boldsymbol{p},t',t)=s} \times [\boldsymbol{E}^R(t'_s)\cdot\boldsymbol{\Upsilon}(\boldsymbol{\pi}(\boldsymbol{p}_s,t'_s)) - \Lambda(\boldsymbol{p}_s,t'_s)] \times \boldsymbol{\Upsilon}^*(\boldsymbol{\pi}(\boldsymbol{p}_s,t_s))e^{-i\Theta(\boldsymbol{p}_s,t'_s,t_s)}, \quad (32)$$

with the saddle points $s = (\boldsymbol{p}_s, t'_s, t_s)$. Equations (29) and (32) denote the main results of this work. With these equations, one can calculate the atomic dipole moment for *any* beam alignment up to the first relativistic correction, which is a unique feature of the GN-SFA.

D. GN-SFA for elliptically polarized plane waves

In this subsection, we will explicitly apply the derived theoretical framework to an elliptically polarized plane wave which is denoted by sub- or superscript e. The respective complex amplitude $\boldsymbol{a}_{\boldsymbol{k}}$ of the vector potential (9) is defined as

$$\boldsymbol{a}^e_{\boldsymbol{k}} = \boldsymbol{a}_0\delta(\boldsymbol{k}-\boldsymbol{k}_0) = \frac{A_0}{\sqrt{1-\epsilon^2}}(\boldsymbol{e}_x + i\epsilon\boldsymbol{e}_y)\delta(\boldsymbol{k}-\boldsymbol{k}_0),$$
$$\boldsymbol{\kappa}^e(t) = i\boldsymbol{k}_0 e^{-i\omega_{k_0}t}.$$

The momentum vector $\boldsymbol{k}_0$ of the resulting laser field is orthogonal to the polarization plane, such that terms that are proportional to $\boldsymbol{k}_0\boldsymbol{A}_{\boldsymbol{k}_0}$ vanish in the nondipole Volkov phase. Explicitly the full nondipole Volkov phase (A2) can be reduced to

$$\Gamma(\boldsymbol{r},t) = \Gamma^e_1(\boldsymbol{r},t) + \Gamma^e_2(\boldsymbol{r},t) \approx \boldsymbol{r}\cdot\left[\boldsymbol{\Gamma}^{e,(r)}_1(t) + \boldsymbol{\Gamma}^{e,(r)}_2(t)\right] + \boldsymbol{p}\cdot\boldsymbol{\Gamma}^{e,(t)}_{\boldsymbol{p}}(t) + \Gamma^{e,(t)}_{\boldsymbol{A}}(t),$$

with $\boldsymbol{p}\cdot\boldsymbol{\Gamma}^e_{\boldsymbol{p}} = \Gamma^{e,(t)}_1$ and $\Gamma_{\boldsymbol{A}} = \Gamma^{e,(t)}_2$. Furthermore, the specific terms $\Gamma^{e,(r/t)}_i$ of the nondipole Volkov phase can be explicitly written as

$$\Gamma^{e,(t)}_1(t) = -\int^t d\tau \frac{\omega_{\boldsymbol{k}_0}}{\eta_{\boldsymbol{k}_0}}\left[\boldsymbol{p}\cdot\boldsymbol{A}^R_{\boldsymbol{k}_0}(\tau)\right],$$
$$\Gamma^{e,(t)}_2(t) = -\int^t d\tau \frac{\omega_{\boldsymbol{k}_0}}{\eta_{\boldsymbol{k}_0}}\frac{\left[\boldsymbol{A}^R_{\boldsymbol{k}_0}(\tau)\right]^2}{2},$$
$$\boldsymbol{\Gamma}^{e,(r)}_1(t) = \frac{\boldsymbol{k}_0}{\eta_{\boldsymbol{k}_0}}\left[\boldsymbol{p}\cdot\boldsymbol{A}^R_{\boldsymbol{k}_0}(\tau)\right],$$
$$\boldsymbol{\Gamma}^{e,(r)}_2(t) = \frac{\boldsymbol{k}_0}{\eta_{\boldsymbol{k}_0}}\frac{\left[\boldsymbol{A}^R_{\boldsymbol{k}_0}(\tau)\right]^2}{2}.$$

With that in mind, we can express the saddle-point momentum $\boldsymbol{p}^e_s$ as

$$\boldsymbol{p}^e_s = \boldsymbol{p}_0 - \frac{\boldsymbol{e}_{\boldsymbol{k}_0}}{c}\int_{t'}^{t} d\tau\left(\frac{\boldsymbol{p}_0\cdot\boldsymbol{A}^R_{\boldsymbol{k}_0}(\tau) + \frac{1}{2}\left[\boldsymbol{A}^R_{\boldsymbol{k}_0}(\tau)\right]^2}{(t-t')}\right), \quad (35)$$

with $\boldsymbol{e}_{\boldsymbol{k}_0}$ as the unit vector of momentum $\boldsymbol{k}_0$ and the saddle-point momentum in the dipole regime $\boldsymbol{p}^e_0 = -\frac{1}{t-t'}\int_{t'}^{t} d\tau\, \boldsymbol{A}^R_{\boldsymbol{k}_0}(\tau)$. Note that the Hessian matrices can be calculated by any computer algebra software and are not further discussed in this work. The remaining variables of the atomic dipole moment can be found in Appendix C. The final expression of the dipole moment for an elliptical polarized monochromatic plane wave is defined as

$$\boldsymbol{D}_e(\omega_q) = -i\sum_s \sqrt{\frac{(2\pi i)^5}{|\boldsymbol{H}^e_{t,t'}(S)||\boldsymbol{H}^e_{\boldsymbol{p}}(S)|}}\Bigg|_{(\boldsymbol{p},t',t)=s} \times \boldsymbol{\Upsilon}^*_e\big(\boldsymbol{\pi}_e(\boldsymbol{p}^e_s,t_s)\big)\left[\boldsymbol{E}^R_{\boldsymbol{k}_0}(t'_s)\cdot\boldsymbol{\Upsilon}_e\big(\boldsymbol{\pi}_e(\boldsymbol{p}^e_s,t'_s)\big)\right] \times e^{-i\Theta_e(\boldsymbol{p}^e_s,t'_s,t_s)}. \quad (36)$$

III. DISCUSSION

In the section above, we motivated and introduced a generalized SFA for high-order harmonic generation which incorporates weakly relativistic effects of arbitrarily spatially structured light fields. The GN-SFA includes relativistic corrections up to $1/c$ such that higher-order terms are neglected.

This section reviews the formal difference between the GN-SFA to the standard nondipole SFA along with an explicit example of a linearly polarized plane wave.

The weakly relativistic regime yields a significant contribution for high intensities and long wavelengths compared to the standard conditions of $I_0 = 10^{14}$ W/cm^2 and $I_p = 15.75$ eV (Ar). For such high intensities and long wavelengths, the effect of ground-state depletion can cause essential deviations. The parameters chosen in this work are selected such that the ground-state depletion can be neglected. Nevertheless, in general, the depletion of the ground state cannot be neglected and needs to be considered.

A. Formal discussion of the GN-SFA

In order to discuss the GN-SFA in general, we compare the specific mathematical structure of this model with other nondipole SFA theories and discuss the newly occurring contributions and the modified ones with regard to their physical interpretation. Even though other nondipole theories exist, we will compare our approach to the model of Kylstra *et al.* [14,15] and refer to it as *standard nondipole SFA*. In the following we highlight the four major differences in the mathematical formulation of the atomic dipole moment (32).

(i) The term $\Lambda(\boldsymbol{p}, t)$ is a unique feature of the GN-SFA and denotes a weakly relativistic correction [$\boldsymbol{\kappa}^{(i)}(t) \propto 1/c$]. $\Lambda(\boldsymbol{p}, t)$ is only nonzero for either noncollinear multibeam alignments or spatially structured beams. From a mathematical perspective this can be interpreted as follows: $\Lambda(\boldsymbol{p}, t)$ vanishes if $\boldsymbol{\kappa}(t)$ is orthogonal to $\boldsymbol{d}(\boldsymbol{\pi}_{\beta 0}^{(i)}(\boldsymbol{p}, t))$, where only the nonrelativistic contributions of $\boldsymbol{d}(\boldsymbol{\pi}_{\beta 0}^{(i)}(\boldsymbol{p}, t))$ need to be considered.

(ii) Instead of the nonrelativistic dipole moment $\boldsymbol{d}(\boldsymbol{p} + \boldsymbol{A}(t))$ the GN-SFA generalizes the transition matrix element to a nondipole or weakly relativistic dipole matrix element $\boldsymbol{\Upsilon}(\boldsymbol{\pi}(\boldsymbol{p}, t))$, which is defined in Eq. (18). Therefore, the general structure remains the same apart from the redefinition of the associated matrix element.

(iii) A remarkable difference with respect to the standard nondipole SFA can be found in the action $S(\boldsymbol{p}, t', t)$ in Eq. (24). As seen from the integrand in Eq. (24) the action cannot be rewritten as the square of the respective kinetical momentum since the square of the relativistic correction of the kinetical momentum that is proportional to $1/c^2$ is not included. The reason for this surprising behavior lies in the initial approach of the GN-SFA where we approximated the full solution of the TDSE for the minimal coupling Hamiltonian (7) to the first relativistic order. In contrast, the standard nondipole SFA constructs the solution of their respective Volkov states by approximating the kinetical momentum up to the first relativistic order which after squaring reveals a contribution in the action that is proportional to $1/c^2$. Especially this contribution seems to be essential for very high wavelengths and field intensities. One approach to solve this issue is to calculate the nondipole Volkov phase up to the second order to include the contributions of the order $1/c^2$. Nevertheless, further investigations in this direction are beyond the scope of this work and offer interesting tasks and questions for further theoretical investigations.

(iv) Perhaps the most important difference between the GN-SFA and the standard nondipole SFA is the spatial structure of the laser field. The standard nondipole SFA restricts the laser field geometry to a specific setup, whereas the GN-SFA does not. Thus our theoretical framework holds for *any* type of light field. Explicitly this means that the standard nondipole SFA is not able to consider multiple noncollinear laser fields and also does not incorporate twisted light fields. The latter, in particular, are interesting due to their topological charge which may induce interesting features like the violation of the selection rules for even and odd harmonics as demonstrated in [24].

B. Explicit application of the GN-SFA

The weakly relativistic correction to the dipole Volkov state in strong-field physics can be interpreted as a finite photon momentum [25] or as the occurrence of a nonvanishing magnetic field that induces a Lorentz force perpendicular to the propagation direction [26]. Overall, these nondipole contributions lead to a decrease in the recombination rate for high-order harmonic generation and therefore a decrease in the harmonic yield. This decrease can also be detected in the high-order harmonic spectrum, where the x component of the GN-SFA dipole moment D_x^{ND} (green dash-dotted) is suppressed compared to the dipole moment of the SFA D_x^D (blue dotted); see Fig. 2. D_z^{ND} (red dashed) refers to the component of the atomic dipole moment in the propagation direction which is directly linked to the nondipole contributions of the laser field. The two global peaks in the components D_x^{ND} and D_z^{ND} at $q = 13000$ and $q = 5500$ are remarkable since they do not occur in the dipole theory. A further feature can be seen when we focus on the high-order harmonic cutoff region in the inset of Fig. 2. One can see that the cutoff is marginally shifted towards lower energy. The standard cutoff law with the maximum photon energy of $E_{\max} = I_p + 3.2U_p$ is nevertheless still valid since the energetic shift is small compared to the cutoff energy itself.

The decrease of the atomic dipole momentum with respect to the intensity I_0 of the laser field and the associated wavelength λ is demonstrated in Fig. 3. Here, we show the ratio R between the coherent sum of the dipole moments calculated from the dipole SFA and the GN-SFA with

$$R = \frac{\left| \int_{q_{min}}^{q_{max}} dq\, \boldsymbol{D}^{ND}(q) \right|}{\left| \int_{q_{min}}^{q_{max}} dq\, \boldsymbol{D}^{D}(q) \right|}, \tag{37}$$

where $\boldsymbol{D}^D(q)$ denotes the atomic dipole momentum in the standard SFA theory and $\boldsymbol{D}^{ND}(q)$ the corresponding atomic dipole moment from the GN-SFA of Eq. (32). In Fig. 3(a) we set the laser field intensity $I_0 = 2 \times 10^{14}$ W/cm^2 for a neon target with ionization potential $I_p = 21.56$ eV, while we consider in Fig. 3(b) the wavelength to be $\lambda = 800$ nm with a doubly ionized lithium target $I_p = 122.45$ eV (Li^{2+}). Note that the ADK ionization rates in both setups are lower than 0.1%. These low ionization rates validate our assumption to neglect the ground-state depletion. The insets show the harmonic spectrum close to the cutoff region for the respective parameters ($I_0 = 4 \times 10^{16}$ W/cm^2, $\lambda = 800$ nm and $I_0 = 2 \times 10^{14}$ W/cm^2, $\lambda = 6800$ nm) denoted by the purple

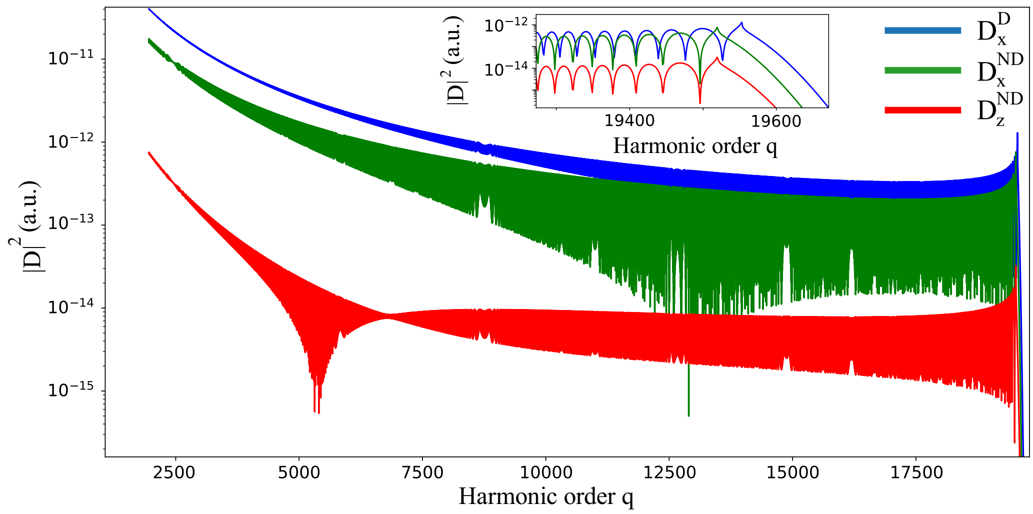

FIG. 2. High harmonic spectrum of a linearly polarized laser field with a rectangular peak envelope $I_0 = 2 \times 10^{14}$ W/cm^2 over one fundamental period T_0, a wavelength of $\lambda = 7400$ nm, and the ionization potential $I_p = 21.56$ eV (Ne). The atomic dipole moment in the x and y direction is calculated within the GN-SFA and denoted by $D_{x/z}^{ND}$, where the atomic dipole moment from the dipole SFA is defined as D_x^D.

star. In both subfigures, we can see the decrease in the ratio R either by the orange curve or in the inset by the decrease in the atomic dipole spectrum.

IV. CONCLUSION

In this work, a generalized version of the well-known nondipole SFA [14] was introduced in order to formally extend high-order harmonic generation to the weakly relativistic regime. To do so, we set up a new framework to define a generalized formula of the atomic dipole moment. In our derivation, the spatial and temporal structure of the laser field is not explicitly specified. This general treatment of the laser field allows one, in contrast to previous approaches, to include noncollinear arbitrarily spatially structured multibeam alignments. The generalized nondipole SFA (GN-SFA) is a rigorously derived theoretical framework and is analytically exact up to the first relativistic order. The atomic dipole moment in the GN-SFA is analogous to the formulation in the standard SFA which allows one to work and think about physical processes and phenomena in a similar way in both theories. As an application, we used the GN-SFA to explicitly discuss the decrease in the high-order harmonic yield for weakly relativistic laser field parameters and compare the results with

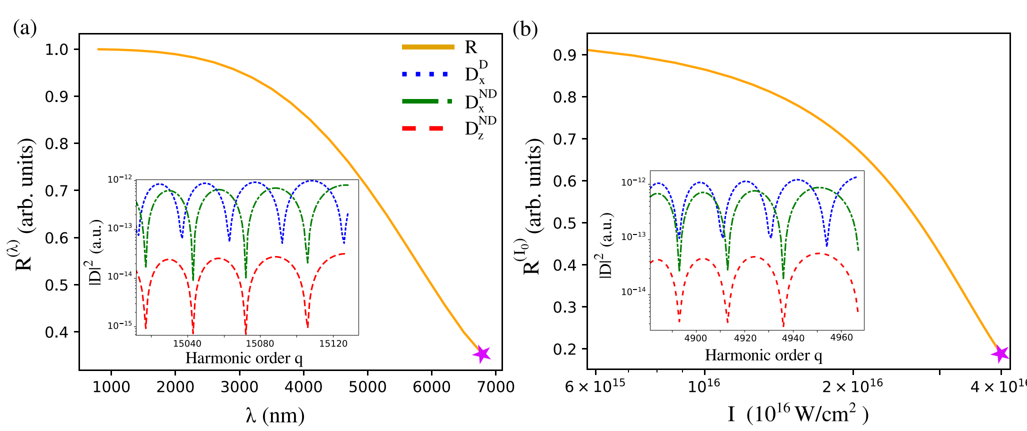

FIG. 3. Visualization of the decrease in the atomic dipole moment with regard to the laser field wavelength λ and the intensity I_0, respectively. We consider a rectangular pulse envelope of the driving beam and a pulse duration of one fundamental period T_0. (a) Wavelength dependent ratio (orange solid) of the coherent sum in Eq. (37) with ionization potential $I_p = 21.56$ eV (Ne). The atomic dipole and nondipole momenta are calculated within the SFA and the GN-SFA [Eq. (36)], respectively. The inset shows the harmonic spectrum close to the respective cutoff region with fixed intensity $I_0 = 2 \times 10^{14}$ W/cm^2 and wavelength $\lambda = 6800$ nm (purple star). D_x^{ND} (green dash-dotted) and D_z^{ND} (red dashed) are associated with the atomic dipole moment calculated within the GN-SFA for the x and z directions, respectively. The atomic dipole moment in the usual dipole SFA is denoted by D_x^D (blue dotted). (b) Atomic dipole moment as a function of the beam intensity I_0 for a wavelength of $\lambda = 800$ nm and the ionization potential $I_p = 122.45$ eV (Li^{2+}). The laser field parameters in the inset are $I_0 = 4 \times 10^{16}$ W/cm^2 and $\lambda = 800$ nm (purple star).

the dipole SFA. Here, we chose the simple case of a linearly polarized plane wave even though more complicated beam geometries can be considered. The results are discussed and compared with regard to the standard nondipole SFA and the dipole SFA.

This work contributes an important step towards a more detailed theoretical understanding of nondipole effects considering the strong-field approximation of high-order harmonic generation. In particular, the decomposition method of the continuum nondipole Volkov states can be generically extended by further correction terms of the nondipole Volkov phase to potentially incorporate crucial contributions that may extend the supported parameter interval.

ACKNOWLEDGMENTS

This work has been funded by the Deutsche Forschungsgemeinschaft (DFG, German Research Foundation) under Project No. 440556973.

APPENDIX A: NONDIPOLE VOLKOV PHASE

The nondipole Volkov phase $\Gamma(\boldsymbol{r}, t)$ is defined in terms of several $\boldsymbol{k}$-dependent functions, which are implicitly defined by the following equations:

$$\boldsymbol{p} \cdot \boldsymbol{A}_{\boldsymbol{k}}^R(t) = \lambda_{\boldsymbol{k}} \cos(u_{\boldsymbol{k}} + \theta_{\boldsymbol{k}}), \tag{A1a}$$

$$-\boldsymbol{k} \cdot \boldsymbol{A}_{\boldsymbol{k}'}^R(t) = \sigma_{\boldsymbol{k}\boldsymbol{k}'} \cos(u_{\boldsymbol{k}'} + \xi_{\boldsymbol{k}\boldsymbol{k}'}), \tag{A1b}$$

$$\frac{1}{4}\boldsymbol{a}_{\boldsymbol{k}} \cdot \boldsymbol{a}_{\boldsymbol{k}'} = \Delta_{\boldsymbol{k}\boldsymbol{k}'}^+ \exp(i\theta_{\boldsymbol{k}\boldsymbol{k}'}^+), \tag{A1c}$$

$$\frac{1}{4}\boldsymbol{a}_{\boldsymbol{k}} \cdot \boldsymbol{a}_{\boldsymbol{k}'}^* = \Delta_{\boldsymbol{k}\boldsymbol{k}'}^- \exp(i\theta_{\boldsymbol{k}\boldsymbol{k}'}^-), \tag{A1d}$$

$$\eta_{\boldsymbol{k}} = \boldsymbol{p} \cdot \boldsymbol{k} - \omega_{\boldsymbol{k}}, \tag{A1e}$$

$$\alpha_{\boldsymbol{k}\boldsymbol{k}'}^{\pm} = \frac{\Delta_{\boldsymbol{k}\boldsymbol{k}'}^{\pm}}{\eta_{\boldsymbol{k}} \pm \eta_{\boldsymbol{k}'}}, \tag{A1f}$$

$$\rho_{\boldsymbol{k}} = \frac{\lambda_{\boldsymbol{k}}}{\eta_{\boldsymbol{k}}}. \tag{A1g}$$

In Eq. (A1a) the product of $\boldsymbol{p}$ and the momentum dependent vector potential $\boldsymbol{A}_{\boldsymbol{k}}^R$ is expressed as a scalar. The same follows in Eq. (A1b) for $\boldsymbol{k} \cdot \boldsymbol{A}_{\boldsymbol{k}'}^R$, while Eqs. (A1c) and (A1d) together are associated with the product $\boldsymbol{A}_{\boldsymbol{k}}^R \cdot \boldsymbol{A}_{\boldsymbol{k}'}^R$. Equation (A1e) introduces a factor which is unique to the GN-SFA and arises in the solution of the TDSE from the nondipole Volkov states, while Eqs. (A1f) and (A1g), on the other hand, are short hand notations.

In terms of these expressions, the complete nondipole Volkov phase has the form

$$\Gamma(\boldsymbol{r}, t) = \sum_{i=1}^{5} \Gamma_i, \quad \Gamma_1(\boldsymbol{r}, t) = \int d^3\boldsymbol{k}\, \rho_{\boldsymbol{k}} \sin(u_{\boldsymbol{k}} + \theta_{\boldsymbol{k}}), \tag{A2a}$$

$$\Gamma_2(\boldsymbol{r}, t) = \int d^3\boldsymbol{k} \int d^3\boldsymbol{k}' [\alpha_{\boldsymbol{k}\boldsymbol{k}'}^+ \sin(u_{\boldsymbol{k}} + u_{\boldsymbol{k}'} + \theta_{\boldsymbol{k}\boldsymbol{k}'}^+) + \alpha_{\boldsymbol{k}\boldsymbol{k}'}^- \sin(u_{\boldsymbol{k}} - u_{\boldsymbol{k}'} + \theta_{\boldsymbol{k}\boldsymbol{k}'}^-)], \tag{A2b}$$

$$\Gamma_3(\boldsymbol{r}, t) = \sum_{\pm} \frac{1}{2} \int d^3\boldsymbol{k} \int d^3\boldsymbol{k}' \sigma_{\boldsymbol{k}\boldsymbol{k}'} \rho_{\boldsymbol{k}} \frac{\sin(u_{\boldsymbol{k}} \pm u_{\boldsymbol{k}'} + \theta_{\boldsymbol{k}} \pm \zeta_{\boldsymbol{k}\boldsymbol{k}'})}{\eta_{\boldsymbol{k}} \pm \eta_{\boldsymbol{k}'}}, \tag{A2c}$$

$$\Gamma_4(\boldsymbol{r}, t) = \sum_{\pm} \int d^3\boldsymbol{k} \int d^3\boldsymbol{k}' \int d^3\boldsymbol{k}'' \sigma_{\boldsymbol{k}\boldsymbol{k}'} \alpha_{\boldsymbol{k}\boldsymbol{k}''}^+ \left(\frac{\sin(u_{\boldsymbol{k}} \pm u_{\boldsymbol{k}'} + u_{\boldsymbol{k}''} + \theta_{\boldsymbol{k}\boldsymbol{k}''}^+ \pm \xi_{\boldsymbol{k}\boldsymbol{k}'})}{\eta_{\boldsymbol{k}} \pm \eta_{\boldsymbol{k}'} + \eta_{\boldsymbol{k}''}} \right), \tag{A2d}$$

$$\Gamma_5(\boldsymbol{r}, t) = \sum_{\pm} \int d^3\boldsymbol{k} \int d^3\boldsymbol{k}' \int d^3\boldsymbol{k}'' \sigma_{\boldsymbol{k}\boldsymbol{k}'} \alpha_{\boldsymbol{k}\boldsymbol{k}''}^- \left(\frac{\sin(u_{\boldsymbol{k}} \pm u_{\boldsymbol{k}'} - u_{\boldsymbol{k}''} + \theta_{\boldsymbol{k}\boldsymbol{k}''}^- \pm \xi_{\boldsymbol{k}\boldsymbol{k}'})}{\eta_{\boldsymbol{k}} \pm \eta_{\boldsymbol{k}'} - \eta_{\boldsymbol{k}''}} \right), \tag{A2e}$$

where Eqs. (A2a) and (A2b) are associated with the standard dipole contributions $\boldsymbol{p} \cdot \boldsymbol{A}_{\boldsymbol{k}}^R$ and $\boldsymbol{A}_{\boldsymbol{k}}^R \cdot \boldsymbol{A}_{\boldsymbol{k}'}^R$. Moreover, Eqs. (A2c)–(A2e) are the nondipole contributions since the $\sigma_{\boldsymbol{k}\boldsymbol{k}'}$ in Eq. (A1b) is proportional to $1/c$.

APPENDIX B: NONDIPOLE SFA

In the following, we give a short derivation of the nondipole matrix element $\boldsymbol{\Upsilon}(\boldsymbol{\pi}(\boldsymbol{p}, t))$ and the dipole matrix element $\boldsymbol{d}(\boldsymbol{\pi}(\boldsymbol{p}, t))$. Both follow directly from the definition of the vector potential:

$$\boldsymbol{A}(\boldsymbol{r}, t) = \boldsymbol{A}(\boldsymbol{r}, t)|_{\boldsymbol{k}\boldsymbol{r}=0} + \boldsymbol{a}_0^R(\boldsymbol{r} \cdot \boldsymbol{\kappa}^R) - \boldsymbol{a}_0^I(\boldsymbol{r} \cdot \boldsymbol{\kappa}^I) + O(1/c^2), \tag{B1}$$

$$\begin{aligned}\boldsymbol{\Upsilon}(\boldsymbol{\pi}(\boldsymbol{p},t)) &= C\int d^3\boldsymbol{r}\, e^{-|r|\sqrt{2I_p}}\boldsymbol{r}\, e^{-i\boldsymbol{r}\cdot[\boldsymbol{p}+\boldsymbol{A}(\boldsymbol{r},t)-\boldsymbol{\Gamma}^{(r)}]}\\ &= C\int d^3\boldsymbol{r}\, e^{-|r|\sqrt{2I_p}}\boldsymbol{r}\, e^{-i\boldsymbol{r}\cdot[\boldsymbol{p}+\boldsymbol{A}(\boldsymbol{r},t)|_{k\cdot r=0}+\boldsymbol{a}_0^R(\boldsymbol{r}\cdot\boldsymbol{\kappa}^R)-\boldsymbol{a}_0^I(\boldsymbol{r}\cdot\boldsymbol{\kappa}^I)-\boldsymbol{\Gamma}^{(r)}]}+O(1/c^2)\\ &= C\int d^3\boldsymbol{r}\, e^{-|r|\sqrt{2I_p}}\boldsymbol{r}\, e^{-i\boldsymbol{r}\cdot[\boldsymbol{p}+\boldsymbol{A}(t)-\boldsymbol{\Gamma}^{(r)}]}\big[1-i(\boldsymbol{r}\cdot\boldsymbol{a}_0^R)(\boldsymbol{r}\cdot\boldsymbol{\kappa}^R)+i(\boldsymbol{r}\cdot\boldsymbol{a}_0^I)(\boldsymbol{r}\cdot\boldsymbol{\kappa}^I)\big]+O(1/c^2),\end{aligned} \tag{B2}$$

$$\Rightarrow \boldsymbol{d}(\boldsymbol{\pi}(\boldsymbol{p},t)) = C\int d^3\boldsymbol{r}\, e^{-|r|\sqrt{2I_p}}\boldsymbol{r}\, e^{-i\boldsymbol{r}\cdot\boldsymbol{\pi}(\boldsymbol{p},t)}. \tag{B3}$$

In Eq. (B1) the definition of the weakly relativistic vector potential is given and inserted in Eq. (B2) followed by an expansion of the exponential which is proportional to $1/c$. Moreover, $\boldsymbol{d}(\boldsymbol{\pi}(\boldsymbol{p},t))$ is the dipole matrix element of hydrogenlike atoms and is defined in Eq. (B3). With this in mind, we can rewrite the nondipole matrix element as

$$\boldsymbol{\Upsilon}(\boldsymbol{\pi}(\boldsymbol{p},t)) = \boldsymbol{d}(\boldsymbol{\pi}(\boldsymbol{p},t)) - iC\int d^3\boldsymbol{r}\, e^{-|r|\sqrt{2I_p}}\boldsymbol{r}\, e^{-i\boldsymbol{r}\cdot\boldsymbol{\pi}(\boldsymbol{p},t)}\big[(\boldsymbol{r}\cdot\boldsymbol{a}_0^R)(\boldsymbol{r}\cdot\boldsymbol{\kappa}^R)-(\boldsymbol{r}\cdot\boldsymbol{a}_0^I)(\boldsymbol{r}\cdot\boldsymbol{\kappa}^I)\big]+O(1/c^2) \tag{B4}$$

$$\begin{aligned}&\Rightarrow \pm(-i)C\int d^3\boldsymbol{r}\, e^{-|r|\sqrt{2I_p}}\boldsymbol{r}\, e^{-i\boldsymbol{r}\cdot\boldsymbol{\pi}(\boldsymbol{p},t)}e^{-i\beta\boldsymbol{r}\cdot\boldsymbol{a}_0^{R/I}}e^{-i\gamma\boldsymbol{r}\cdot\boldsymbol{\kappa}^{R/I}}(\boldsymbol{r}\cdot\boldsymbol{a}_0^{R/I})(\boldsymbol{r}\cdot\boldsymbol{\kappa}^{R/I})\big|_{\beta=\gamma=0}\\ &= \pm i\partial_\beta\partial_\gamma C\int d^3\boldsymbol{r}\, e^{-|r|\sqrt{2I_p}}\boldsymbol{r}\, e^{-i\boldsymbol{r}\cdot\boldsymbol{\pi}(\boldsymbol{p},t)}e^{-i\beta\boldsymbol{r}\cdot\boldsymbol{a}_0^{R/I}}e^{-i\gamma\boldsymbol{r}\cdot\boldsymbol{\kappa}^{R/I}}\big|_{\beta=\gamma=0}\\ &= \pm i\partial_\beta\partial_\gamma \boldsymbol{d}\big(\boldsymbol{\pi}(\boldsymbol{p},t)+\beta\boldsymbol{r}\cdot\boldsymbol{a}_0^{R/I}+\gamma\boldsymbol{r}\cdot\boldsymbol{\kappa}^{R/I}\big)\big|_{\beta=\gamma=0}\\ &= \pm i\partial_\beta\partial_\gamma \boldsymbol{d}\big(\boldsymbol{\pi}_{\beta\gamma}^{R/I}(\boldsymbol{p},t)\big)\big|_{\beta=\gamma=0}\end{aligned}$$

$$\Rightarrow \boldsymbol{\Upsilon}(\boldsymbol{\pi}(\boldsymbol{p},t)) = \boldsymbol{d}(\boldsymbol{\pi}(\boldsymbol{p},t)) + i\partial_\beta\partial_\gamma\big[\boldsymbol{d}\big(\boldsymbol{\pi}_{\beta\gamma}^R(\boldsymbol{p},t)\big)-\boldsymbol{d}\big(\boldsymbol{\pi}_{\beta\gamma}^I(\boldsymbol{p},t)\big)\big]+O(1/c^2). \tag{B5}$$

In the calculation step from Eq. (B4) to Eq. (B5), we introduced the dummy variables β and γ in the argument of a complex exponential to express the second factor of Eq. (B2) as the derivative of the complex exponential with regard to the dummy variables. Due to this reformulation, we can define the nondipole matrix element as done in Eq. (B5):

$$\hat{\partial}_\beta \boldsymbol{d}\big(\boldsymbol{\pi}_{\beta\gamma}^{(i)}\big)\big|_{\beta=\gamma=0} = \frac{2^{19/4}I_p^{5/4}}{\pi}\left(\frac{\boldsymbol{a}_0^i}{(\boldsymbol{\pi}^2+2I_p)^3}-6\frac{\boldsymbol{\pi}(\boldsymbol{\pi}\cdot\boldsymbol{a}_0^i)}{(\boldsymbol{\pi}^2+2I_p)^4}\right), \tag{B6}$$

$$\hat{\partial}_\beta\hat{\partial}_\gamma \boldsymbol{d}\big(\boldsymbol{\pi}_{\beta\gamma}^{(i)}\big)\big|_{\beta=\gamma=0} = -\frac{2^{19/4}I_p^{5/4}}{\pi}\left(6\frac{\boldsymbol{\kappa}^i(\boldsymbol{\pi}\cdot\boldsymbol{a}_0^i)+\boldsymbol{a}_0^i(\boldsymbol{\pi}\cdot\boldsymbol{\kappa}^i)+\boldsymbol{\pi}(\boldsymbol{\kappa}^i\cdot\boldsymbol{a}_0^i)}{(\boldsymbol{\pi}^2+2I_p)^4}-48\frac{\boldsymbol{\pi}(\boldsymbol{\pi}\cdot\boldsymbol{\kappa}^i)(\boldsymbol{\pi}\cdot\boldsymbol{a}_0^i)}{(\boldsymbol{\pi}^2+2I_p)^5}\right). \tag{B7}$$

In these two equations, we explicitly derived the terms that occur in the nondipole matrix element (18) and the nondipole component of the electric field (22) from the nondipole ionization amplitude (21) with $\boldsymbol{\pi}\equiv\boldsymbol{\pi}_{00}$.

APPENDIX C: NONDIPOLE SFA FOR ELLIPTICAL POLARIZED PLANE WAVES

The remaining variables for an elliptically polarized plane wave are easily calculated from their general definition as

$$\boldsymbol{A}_{\boldsymbol{k}_0}^R(t) = \frac{A_0}{\sqrt{1+\epsilon^2}}\begin{pmatrix}\cos(\omega t)\\ \epsilon\,\sin(\omega t)\\ 0\end{pmatrix}, \tag{C1}$$

$$\boldsymbol{E}_{\boldsymbol{k}_0}^R(t) = -\hat{\partial}_t\boldsymbol{A}_{\boldsymbol{k}_0}^R(t), \tag{C2}$$

$$\boldsymbol{\pi}(\boldsymbol{p},t) = \boldsymbol{p}+\boldsymbol{A}_{\boldsymbol{k}_0}^R(t)-\frac{\boldsymbol{k}_0}{\eta_{\boldsymbol{k}_0}}\left(\big[\boldsymbol{p}\cdot\boldsymbol{A}_{\boldsymbol{k}_0}^R(t)\big]+\frac{\big[\boldsymbol{A}_{\boldsymbol{k}_0}^R(t)\big]^2}{2}\right), \tag{C3}$$

$$\boldsymbol{\Upsilon}(\boldsymbol{\pi}(\boldsymbol{p},t)) = \boldsymbol{d}(\boldsymbol{\pi}(\boldsymbol{p},t)) - 6\frac{\boldsymbol{e}_{\boldsymbol{k}_0}}{c}\frac{\big[\boldsymbol{d}(\boldsymbol{\pi}(\boldsymbol{p},t))\cdot\boldsymbol{E}_{\boldsymbol{k}_0}^R(t)\big]}{\boldsymbol{\pi}(\boldsymbol{p},t)^2+2I_p}, \tag{C4}$$

$$\Lambda(\boldsymbol{p},t') = 0, \tag{C5}$$

$$\Theta(\boldsymbol{p}_s,t',t) = \int_{t'}^{t} d\tau\left[\frac{\boldsymbol{p}_s^2}{2}-\frac{\omega_{\boldsymbol{k}_0}}{\eta_{\boldsymbol{k}_0}}\left(\big[\boldsymbol{p}_s\cdot\boldsymbol{A}_{\boldsymbol{k}_0}^R(\tau)\big]+\frac{\big[\boldsymbol{A}_{\boldsymbol{k}_0}^R(\tau)\big]^2}{2}\right)+I_p\right]-\omega_q t, \tag{C6}$$

where Eqs. (C1) and (B2) denote the real part of the momentum-dependent vector potential and electric field, respectively. Equation (C3) can be interpreted as the kinetic momentum of the continuum electron. Where in Eq. (C4) the explicit form of the nondipole matrix element is defined, the weakly relativistic correction to the nondipole ionization amplitude in Eq. (C5) vanishes. Finally the complex exponential incorporating the action in Eq. (24) can be read off in Eq. (C6).

[1] P. Agostini, F. Fabre, G. Mainfray, G. Petite, and N. K. Rahman, Free-Free Transitions Following Six-Photon Ionization of Xenon Atoms, Phys. Rev. Lett. **42**, 1127 (1979).

[2] G. G. Paulus, W. Nicklich, H. Xu, P. Lambropoulos, and H. Walther, Plateau in Above Threshold Ionization Spectra, Phys. Rev. Lett. **72**, 2851 (1994).

[3] B. Böning, W. Paufler, and S. Fritzsche, Polarization-dependent high-intensity Kapitza-Dirac effect in strong laser fields, Phys. Rev. A **101**, 031401(R) (2020).

[4] P. B. Corkum, Plasma Perspective on Strong Field Multiphoton Ionization, Phys. Rev. Lett. **71**, 1994 (1993).

[5] A. McPherson, G. Gibson, H. Jara, U. Johann, T. S. Luk, I. A. McIntyre, K. Boyer, and C. K. Rhodes, Studies of multiphoton production of vacuum-ultraviolet radiation in the rare gases, J. Opt. Soc. Am. B **4**, 595 (1987).

[6] M. Ferray, A. L'Huillier, X. F. Li, L. A. Lompre, G. Mainfray, and C. Manus, Multiple-harmonic conversion of 1064 nm radiation in rare gases, J. Phys. B: At., Mol., Opt. Phys. **21**, L31 (1988).

[7] B. Minneker, B. Böning, A. Weber, and S. Fritzsche, Torus-knot angular momentum in twisted attosecond pulses from high-order harmonic generation, Phys. Rev. A **104**, 053116 (2021).

[8] A. Weber, B. Böning, B. Minneker, and S. Fritzsche, Generation of elliptically polarized high-order harmonic radiation with bi-elliptical two-color laser beams, Phys. Rev. A **104**, 063118 (2021).

[9] E. Pisanty, G. J. Machado, V. Vicuña-Hernández, A. Picón, A. Celi, J. P. Torres, and M. Lewenstein, Knotting fractional-order knots with the polarization state of light, Nat. Photon. **13**, 569 (2019).

[10] K. J. Schafer and K. C. Kulander, High Harmonic Generation from Ultrafast Pump Lasers, Phys. Rev. Lett. **78**, 638 (1997).

[11] M. Lewenstein, P. Balcou, M. Y. Ivanov, A. L'Huillier, and P. B. Corkum, Theory of high-harmonic generation by low-frequency laser fields, Phys. Rev. A **49**, 2117 (1994).

[12] H. R. Reiss, Effect of an intense electromagnetic field on a weakly bound system, Phys. Rev. A **22**, 1786 (1980).

[13] D. M. Wolkow, Über eine klasse von lösungen der diracschen gleichung, Z. Phys. **94**, 250 (1935).

[14] N. J. Kylstra, R. M. Potvliege, and C. J. Joachain, Photon emission by ions interacting with short intense laser pulses: beyond the dipole approximation, J. Phys. B: At., Mol., Opt. Phys. **34**, L55 (2001).

[15] C. C. Chirilă, N. J. Kylstra, R. M. Potvliege, and C. J. Joachain, Nondipole effects in photon emission by laser-driven ions, Phys. Rev. A **66**, 063411 (2002).

[16] K. Amini, J. Biegert, F. Calegari, A. Chacón, M. F. Ciappina, A. Dauphin, D. K. Efimov, C. F. de Morisson Faria, K. Giergiel, P. Gniewek *et al.*, Symphony on strong field approximation, Rep. Prog. Phys. **82**, 116001 (2019).

[17] D. Bauer, D. B. Milošević, and W. Becker, Strong-field approximation for intense-laser–atom processes: The choice of gauge, Phys. Rev. A **72**, 023415 (2005).

[18] W. Becker and D. Milošević, A gauge-covariant derivation of the strong-field approximation, Laser Phys. **19**, 1621 (2009).

[19] E. Pisanty, D. D. Hickstein, B. R. Galloway, C. G. Durfee, H. C. Kapteyn, M. M. Murnane, and M. Ivanov, High harmonic interferometry of the Lorentz force in strong mid-infrared laser fields, New J. Phys. **20**, 053036 (2018).

[20] M. Klaiber, K. Z. Hatsagortsyan, and C. H. Keitel, Gauge-invariant relativistic strong-field approximation, Phys. Rev. A **73**, 053411 (2006).

[21] Y. V. Vanne and A. Saenz, Generalized gauge-invariant formulations of the strong-field approximation, Phys. Rev. A **79**, 023421 (2009).

[22] L. Rosenberg and F. Zhou, Generalized Volkov wave functions: Application to laser-assisted scattering, Phys. Rev. A **47**, 2146 (1993).

[23] B. Böning, W. Paufler, and S. Fritzsche, Nondipole strong-field approximation for spatially structured laser fields, Phys. Rev. A **99**, 053404 (2019).

[24] B. Wang, L. Li, Y. Zhang, C. Zhai, X. Zhu, P. Lan, and P. Lu, Non-dipole effect in vortex high-order harmonic generation, J. Phys. B: At., Mol., Opt. Phys. **53**, 215601 (2020).

[25] B. Böning, Ph.D. thesis, Dissertation, Friedrich-Schiller-Universität Jena, 2020.

[26] A. Hartung, S. Eckart, S. Brennecke, J. Rist, D. Trabert, K. Fehre, M. Richter, H. Sann, S. Zeller, K. Henrichs *et al.*, Magnetic fields alter strong-field ionization, Nat. Phys. **15**, 1222 (2019).